International Journal of Mining Science and Technology xxx (xxxx) xxx

Contents lists available at ScienceDirect

International Journal of Mining Science and Technology

journal homepage: www.elsevier.com/locate/ijmst

Comparison of laboratory and field electrical resistivity measurements of a gypsum rock for mining prospection applications

Chiara Caselle *, Sabrina Bonetto, Cesare Comina

Department of Earth Science (DST), Torino University, Torino 10125, Italy

ARTICLE INFO

Article history:
Received 26 June 2018
Received in revised form 16 January 2019
Accepted 25 September 2019
Available online xxxx

Keywords:
Gypsum rock
Electrical resistivity
Saturation
Porosity
Archie
ERT
Quarry

ABSTRACT

Geophysical surveys are frequently applied in mining prospection to detect the presence and volume of ore bodies of different nature. Particularly, in gypsum ore bodies exploitation, electrical resistivity measurements are usually the most used methodology. However, it has been observed that different electrical resistivity values can be obtained depending on geometrical features and composition of gypsum. Indeed, electrical resistivity of gypsum rocks depends on several parameters, such as gypsum purity, nature of secondary minerals, porosity, saturation and interstitial fluid properties. Saturation and hydrogeological setting, in particular, were recognized as the most influencing parameters. Hydrogeological conditions of gypsum rock masses are also very relevant for exploitability, safety conditions and economic feasibility and should be accurately known during the prospection and planning phases of the quarries. In this work, a relationship between electrical resistivity and saturation degree of gypsum is proposed. The possibility to estimate gypsum porosity with the use of this relationship is also investigated. The reliability of laboratory measurements is finally verified in comparison with field and modelled resistivity data. The reported results underline the potentiality of the proposed approach to obtain a reliable characterization of the studied ore body.

1. Introduction

Electrical resistivity defines the propensity of a material to be crossed by electrical current. In geological materials the electrical resistivity may depend on both intrinsic parameters, such as mineralogical composition, porosity and clay content, and state variables, such as water saturation and properties of interstitial fluid. Geoelectrical surveys based on the measure of electrical resistivity, such as ERT (Electrical Resistivity Tomography), have been extensively used for the location and description of geometrical and compositional features of geological bodies. In mining planning, geoelectrical surveys are frequently used to integrate local information obtained from boreholes and to reconstruct the areal extension of the ore bodies e.g. [1–5].

Among the most studied ore bodies, gypsum (dehydrate calcium sulphate, $CaSO_4{\cdot}2H_2O$) has several potential applications in the construction industry. Gypsum rocks are exploited in several areas of the world by both open pit and underground quarries. Usually, gypsum rocks have a significantly higher electrical resistivity with respect to clay and marl sediments that surround it in most geological frameworks. The application of geoelectrical surveys to gypsum ore bodies identification has been therefore successfully proposed in the scientific literature [6–10].

Nevertheless, gypsum formations have a high geological variability. Gypsum can be present in nature in a wide combination of facies, with different grain sizes, porosity, moisture contents and percentage of clay minerals [29–32,34,35]. Most of these parameters may influence electrical resistivity measurements. Several authors report on the electrical resistivity values measured over gypsum rocks evidencing a high variability in the results [6,7,11,12]. Measured resistivities span in the 10–1200 Ω m range. Lower values are usually associated to unconsolidated gypsum sediments with relevant percentages of marls in the formation [13]. Higher values correspond to the presence of anhydrite within the gypsum formation [6]. The wide range of values confirms the variability of resistivity as a consequence of the high natural variability of the material.

Particularly, in the study by Guinea et al. [9], a strong dependence of gypsum electrical resistivity on mineralogical composition and on the presence and the percentage of lutites (which included, in the specific case, carbonates, quartz and other minor accompanying minerals) was evidenced. This dependence was investigated through modelled, laboratory and field data,

* Corresponding author.
E-mail address: chiara.caselle@unito.it (C. Caselle).

https://doi.org/10.1016/j.ijmst.2019.09.002
2095-2686/

proposing an electrical classification of gypsum as a function of gypsum content (Table 1). On the basis of this classification, it may be possible to indirectly retrieve the gypsum purity of an orebody from the resistivity data. The complexity of the problem was further deepened, considering the variation of electrical resistivity in the system gypsum-anhydrite-lutitic matrix in [10].

All the cited works agree in establishing a limit resistivity value (around 1000 Ω m) above which the gypsum percentage can be considered satisfactory for exploitation (i.e. above 80%). Nevertheless, the effect of water saturation is neglected in these studies, considering the influence of water not relevant on the result, given the low porosity and permeability of gypsum. The influence of the soil humidity on ERT surveys for the identification of underground caves in gypsum deposits was investigated in [14]. The moisture content of the soil was evaluated as a function of meteorological conditions, concluding that the resolution of ERT improves if the soil is humid. However, also in this case, the saturation of gypsum body itself is not considered as a relevant parameter. The increase in resistivity in a gypsum deposit was explained in the study by Ball et al., considering three hypotheses: the increase of porosity of gypsum, the presence of interbedded limestones or the decrease in water content. Even if they did not have enough elements to check these hypotheses, three important elements that may influence the electrical resistivity of gypsum rocks were highlighted [7].

Besides the potential influence of saturating water on electrical resistivity, the hydrogeological conditions of the gypsum rock masses are often very relevant for exploitability, safety conditions and economic feasibility of the excavations. Even if the primary permeability of gypsum is usually very low, this material can be often associated to karst aquifers. The features of these aquifers can be extremely different, ranging from systems with dominant conduit drainage to systems with interconnected conduit drainage and with dispersive circulation. This last condition can be assimilated to porous granular aquifers [15]. The phenomenon of karst circulation and the presence of water inside the orebody are two of the main causes of risk in gypsum exploitation, particularly in underground quarries, outlining scenarios of potential geological hazard [16,36]. The possibility to know in advance the saturation conditions and saturation distribution of a gypsum orebody with non-destructive and cheap analyses, like ERT, represents therefore an important goal in mining prospection.

Water saturation is therefore, in our opinion, one of the most important parameters for a reliable analysis of electrical resistivity measurements over gypsum orebodies. This parameter has been not particularly investigated so far in literature studies. In this work a correlation between water saturation of gypsum rock and electrical resistivity is studied. Porosity and gypsum content of natural gypsum samples from a quarry in the Monferrato area (Piedmont, NW Italy) were determined by laboratory tests. Samples were then brought to different saturation conditions and the resulting electrical resistivity variations were measured. A relationship between saturation and resistivity was obtained, considering the proper resistivity for the interstitial fluid. This relationship allows, moreover, an estimation of the porosity of the material, which has a significant influence on the strength and deformation features of the rock, conditioning the mining design e.g. [17]. The reliability of the proposed relationship was also evaluated in comparison with field ERT data. Stratigraphy and saturation conditions at the field scale were confirmed by the use of laboratory data and modelled resistivity data calibrated on the laboratory outcomes.

Table 1
Geolectrical classification of gypsum rocks, from Guinea et al. [9].

Type of gypsum rock	Gypsum purity (%)	Resistivity (Ωm)
Pure gypsum	75–100	700–1000
Transitional gypsum (dirty gypsum)	55–75	100–700
Lutites and gypsum-rich lutites	0–55	10–100

2. Geological framework

The test site is located in the Monferrato area (Piedmont, NW Italy, Fig. 1a). In the area, significant gypsum ore bodies are present and have been extensively exploited for several decades. Gypsum in the Monferrato area has been deposited in Late Miocene during the so-called "Messinian Salinity Crisis", a period of anomalous salinity conditions that involved the entire Mediterranean basin [18]. The base of the stratigraphic succession consists of clay and carbonate fine sediments (Sant'Agata Fossili Marls, Fig. 1b).

The exploited gypsum belongs to the lower part of the first gypsum unit (PLG–Primary Lower Gypsum unit–Fig. 1b) which is organized in four thick gypsum layers alternated with marl layers. The relevant thickness of these gypsum layers allow an effective exploitation. At their top, the unit presents a more dense alternation of gypsum and marl. Towards the top of the unit, the presence of gypsum is limited to single gypsum crystals dispersed in a matrix of marl or to thin layers within the marl sediments. In the deepest parts of the basin, the PLG unit is locally redeposited as chaotic body (RLG–resedimented gypsum unit–Fig. 1b). At the top of PLG and RLG units, geological formations are mainly constituted by marls and clays.

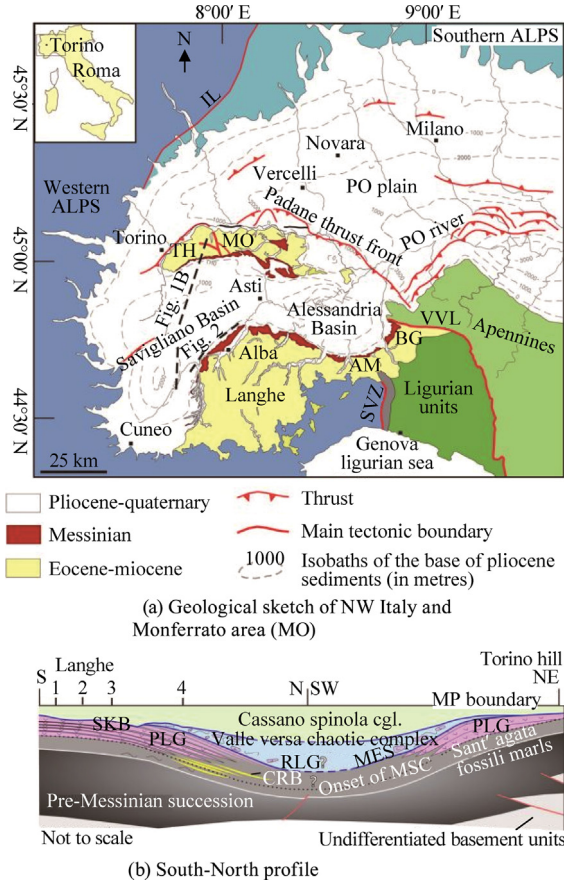

Fig. 1. Schematic geological representation of NW Italy. In Fig. 1, IL is Insubric Line; TH is Torino Hill; AM is Alto Monferrato; BG is Borbera Grue; VVL is Villarvernia Varzi Line; SVZ is Sestri Voltaggio shear zone; SKB is Sturani key bed; PLG is primary lower gypsum; RLG is resedimented lower gypsum [19].

Please cite this article as: C. Caselle, S. Bonetto and C. Comina, Comparison of laboratory and field electrical resistivity measurements of a gypsum rock for mining prospection applications, International Journal of Mining Science and Technology, https://doi.org/10.1016/j.ijmst.2019.09.002

The hydrogeological circulation in the area generated the development of significant karst circuits. In particular, the test site is interested by a "system with dispersive circulation": gypsum rock is intensely fractured, has a rather low general permeability and does not show preferential drainage paths or karst conduits but tends to create a water table level, similarly to classical piezometric surfaces in porous aquifers [15]. Measurements of water electrical conductibility performed in several boreholes and natural springs, show values ranging between 2.60 and 4.00 mS/cm [15,20].

Several survey holes were drilled in the test site (Fig. 2a). Drilling was performed with core destruction in the cap sediments and in the upper part of the PLG unit. In these parts of the drilled column, the limited content of gypsum in the prevalently marl sediments does not represent a potentially exploitable unit. Conversely, the entire thickness of the gypsum orebody was sampled with continuous cores, with the possibility of a complete reconstruction of the local stratigraphy. Information from all of the performed soundings is quite consistent: the orebody consists of 3 macrocrystalline gypsum layers and 1 microcrystalline gypsum layer separated by thin marl layers with thickness of 1–2 m. Gypsum layers present mean thickness of 10, 14, 13 and 8 m from the bottom to the top (Fig. 2b). The top of the succession has an average depth of 25 m from the ground surface.

3. Methods

3.1. Laboratory measurements

Samples from the drilling cores were collected for laboratory tests. Fig. 2b shows the position of the samples along the stratigraphic column: 3 samples of microcrystalline gypsum and 2 samples of macrocrystalline gypsum were selected and denominated m1, m2 and m3 and M4 and M5 respectively (Fig. 3). The macrocrystalline samples are constituted by big elongated selenite gypsum crystals, with average size of 2 cm × 5 cm. Longer crystals can even reach 8–10 cm. The growth direction of the crystals is typically vertical and perpendicular to the bed stratification. The microcrystalline samples have finer-grained gypsum crystals, with average size of about 1 mm. The most typical facies in this layer is the "branching selenite". It consists of elongated selenite crystals with long axis inclined or oriented horizontally, grouped into decimetre-large irregular nodules, and lenses, separated by thin fine-grained carbonate or gypsum laminae [21].

Diameter and length of each collected sample were measured with a caliber and each sample volume was retrieved. Samples were then saturated in tap water (with an electrical conductivity of 0.5 mS/cm) for a period of at least 72 h. Weight variations were monitored during the saturation period to decide when to interrupt it. Because of the high gypsum solubility in water, after an initial mass increase due to the saturation of intercrystal voids, the sample mass tends to decrease due to dissolution. After 72 h, samples were considered completely saturated [22]. An electrical conductivity of 2.15 mS/cm was measured for the saturating water at the end of the saturation phase. The increase in water conductivity can be related to the partial dissolution of the gypsum samples and to the passage in solution of dissolved salts coming from the gypsum samples themselves.

Starting from these saturated samples, different degrees of saturation were then obtained with short time heating intervals (2 h) at low temperatures (40 °C). Temperatures higher than 40–60 °C could indeed bring to the dehydration of the crystalline structure of gypsum, changing the mineralogical nature of the material. Samples were considered dry after a final period in oven of 12 h at 60 °C. The total mass of water in the saturated samples was calculated as weight difference with the dry samples. The porosity of each sample was then retrieved. The degree of saturation of each heating step was also calculated for each sample (Table 2). It can be observed that, with the adopted methodology, a wide range of saturation degrees was obtained for each sample, approximately each 10% degree of saturation.

In order to estimate fluid conductivity changes during the tests, samples of saturating water at the end of the saturation phase were heated in oven togheter with overabundant gypsum material with the same time schedule used for the rock samples. Conductivity was measured at the end of each step. The conductivity values, reported in Table 2, show an increasing trend between 2.20 and 4.00 mS/cm, which reflects the increased solubility of gypsum with

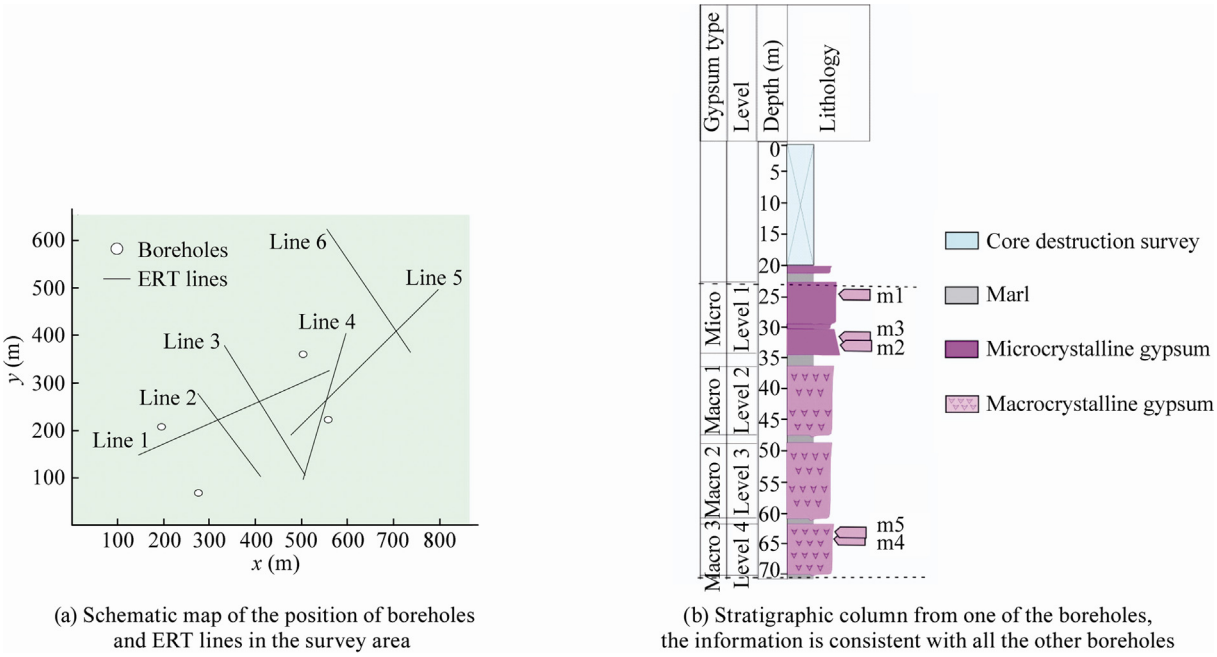

(a) Schematic map of the position of boreholes and ERT lines in the survey area

(b) Stratigraphic column from one of the boreholes, the information is consistent with all the other boreholes

Fig. 2. Geometrical representation of ERT lines, boreholes and samples depth.

Please cite this article as: C. Caselle, S. Bonetto and C. Comina, Comparison of laboratory and field electrical resistivity measurements of a gypsum rock for mining prospection applications, International Journal of Mining Science and Technology, https://doi.org/10.1016/j.ijmst.2019.09.002

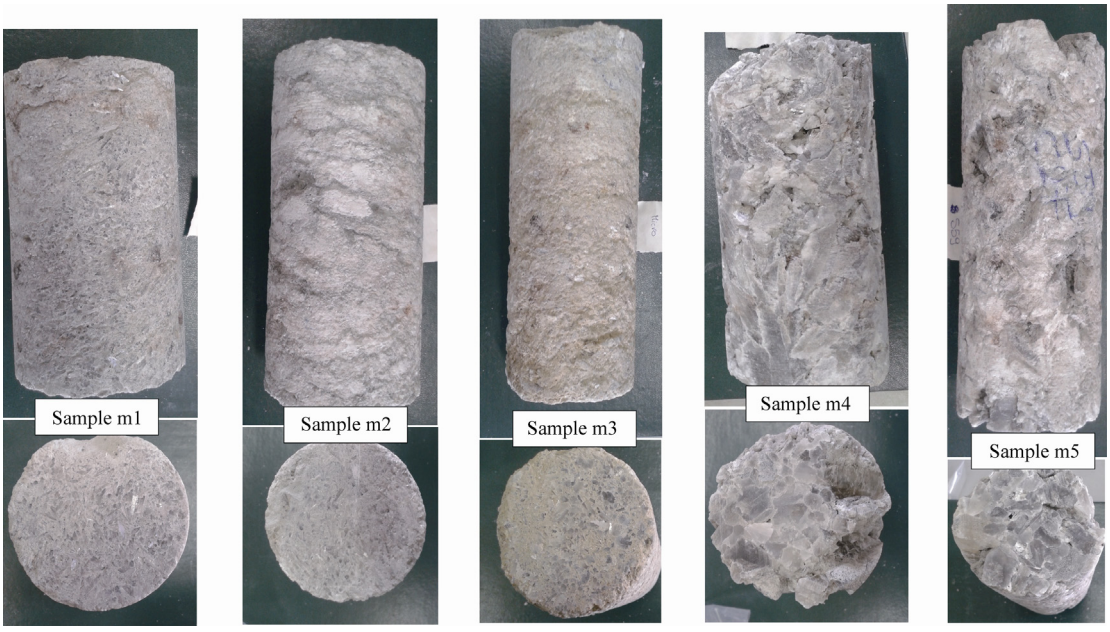

Fig. 3. Photographical images of the samples.

Table 2
Heating steps, relative saturation percentages for each samples and water conductivity.

Time (h)	T (°C)	m1 Saturation (%)	m2 Saturation (%)	m3 Saturation (%)	M4 Saturation (%)	M5 Saturation (%)	Water conductivity (mS/cm)
0	40	100.00	100.00	100.00	100.00	100.00	2.15
2	40	93.05	94.06	94.14	79.41	69.09	2.16
2	40	77.81	81.45	84.37	69.12	64.61	2.18
2	40	67.88	68.09	74.11	52.10	52.70	2.22
2	40	50.33	46.01	51.77	14.92	16.69	2.24
3	40	46.69	42.67	48.47	13.87	12.83	2.33
3	40	28.48	24.12	28.94	5.25	4.33	2.34
4	40	21.85	19.11	23.57	4.41	2.47	2.26
4	40	15.23	8.16	12.45	1.89	0.31	2.61
12	50	4.64	0.74	3.30	1.26	0.31	3.41
12	60	0	0	0	0	0	4.00

temperature. Particularly, the highest conductivity values are observed near the dry samples condition. The obtained conductivity values are similar to the ones measured in underground waters within gypsum orebodies in the area [15,20].

Electrical resistivity of each sample was measured after each heating step. Measurements were carried out using an on-proper designed device with 4 brass electrodes, 0.03 m spaced, in a Wenner quadripole acquisition geometry (Fig. 4a), connected to a Syscal-Pro (Iris instruments) acquisition system. This measuring device has been developed following standard methods for the determination of surface resistivity in concrete samples [23]. Results with the use of similar devices already showed a correlation of surface resistivity measurements and saturation levels [24].

Before performing the measurements, the device was tested and calibrated on water samples with parallel acquisitions with a standard conductivity meter. Different water solutions, with increasing content of NaCl (from distilled water to saturated solution), were adopted. The calibration results (Fig. 4b) show higher uncertainties for higher resistivity values (lower saline concentration). This may be partially due to difficulties in injecting the

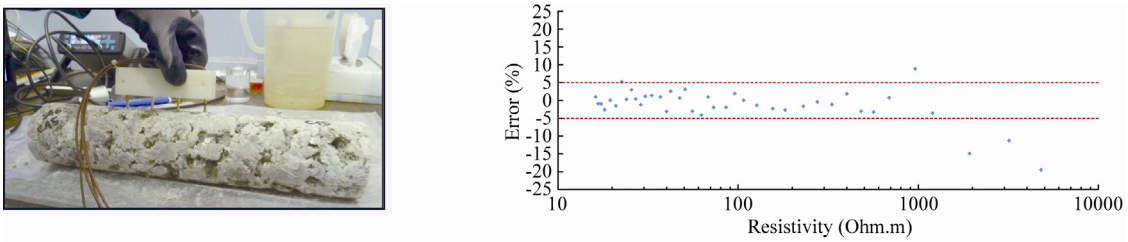

(a) Electrical resistivity measure on a macrocrystalline gypsum sample

(b) Error in measured resistivity with the proposed device with respect to the conductivity meter, in water solutions with different concentration levels

Fig. 4. Methodology for the measure of electrical resistivity on samples.

Please cite this article as: C. Caselle, S. Bonetto and C. Comina, Comparison of laboratory and field electrical resistivity measurements of a gypsum rock for mining prospection applications, International Journal of Mining Science and Technology, https://doi.org/10.1016/j.ijmst.2019.09.002

current at electrodes, in order to perform stable measurements, in very resistive environments (i.e. above 1000 Ω m). On the other hand, for lower resistivity values, the data are very similar (i.e. below 5% difference). Each resistivity measurement on the samples was repeated 3 to 5 times, also inverting the current flow direction, in order to have information about the experimental uncertainty.

At the end of the resistivity measurements, the mineralogical content of the samples was also determined. Gypsum content was measured for each sample with the thermogravimetric method, following the methodology described in study by Porta [25]. The nature of non-gypsum minerals was also investigated with XRPD (X-Ray Powder Diffraction) analyses. With this aim, 0.5 g of material were crushed with a mortar and diluted in water, creating a solution with a concertation lower than gypsum solubility (2 g/L). The filtered solid residual of this solution was deposited for the RX analysis, in order to study the insoluble minerals without the interference of gypsum spectrum.

3.2. Field measurements

Six ERT profiles were acquired in the test site, covering a total area of about 6 km^2 (Fig. 2a). Data were acquired with a Syscal-Pro (Iris instruments) acquisition system and a Wenner-Schulumberger quadripole configuration, in order to assure a good compromise between lateral resolution and investigation depth. Each line was composed of 48 electrodes with different spacings (from 5 to 10 m) depending on the logistic of the site. A total of 871 potential measurements were collected along each line. Data inversion was performed with Res2dInv software [26]. Before the inversion process, some pre-processing operations on the data were performed, with the aim to evaluate their quality and to eliminate unreliable data. The measured data were analyzed from statistical point of view to remove higher uncertainty measurements. In particular, measures with experimental uncertainty higher than 5% and values considered affected by local heterogeneities were eliminated.

4. Results

4.1. Laboratory measurements

Fig. 5a and b show the results of electrical resistivity measurements on gypsum samples as a function of their degree of saturation. Measured resistivity values were normalized with respect to the water resistivity, obtaining the formation factor ($F = \rho/\rho_w$). Each obtained data series was then interpolated with the Archie relationship [27]. This relationship, largely used in scientific literature e.g. [28], suggests the existence of direct proportionality between resistivity of a material (ρ) and resistivity of the fluid that permeates the pores (ρ_w), with a correlation factor F (Formation Factor) depending on the porosity (φ) and on the saturation (S) conditions:

$$F = \rho/\rho_w = (a\varphi^{-m}S^{-k})$$

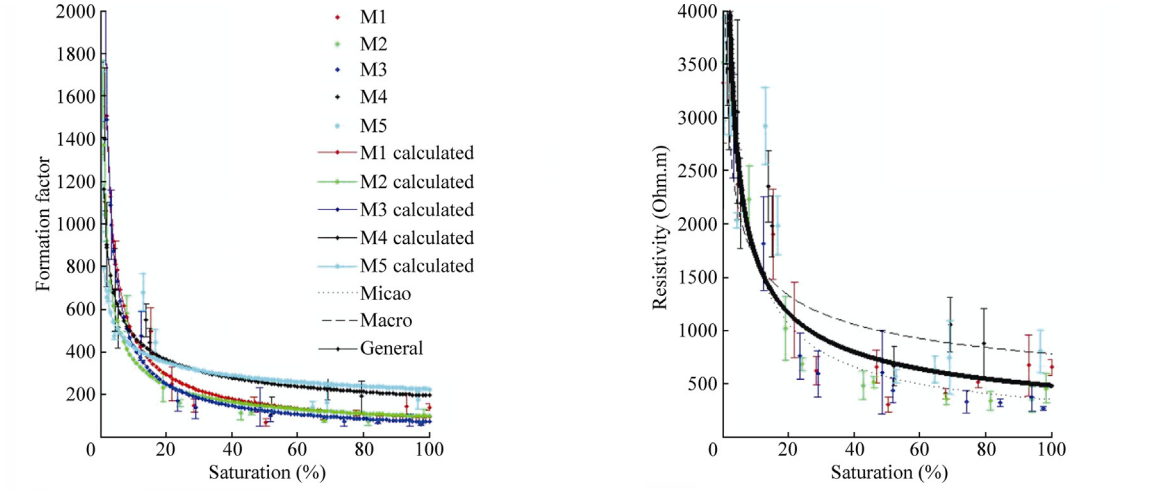

(a) Formation Factor as a function of the saturation conditions. Interpolated curves with Archie Formula for each tested sample are also reported

(b) Resistivity data as a function of the saturation conditions compared with the mean Archie curves for microcrystalline gypsum, macrocrystalline gypsum and for the entire dataset

Fig. 5. Results of electrical resistivity measures on samples with different saturation degrees.

Table 3
a, *m* and *k* parameters for each sample and relative R^2 values for each curve.

Item	Item	*a*	*m*	*k*	R^2
Microcrystalline gypsum	m1	2.254	1.190	0.712	0.9182
	m2	2.341	1.431	0.575	0.9803
	m3	2.273	1.365	0.775	0.9757
	Mean	2.290	1.329	0.687	
	St Dev	0.046	0.124	0.102	
Macrocrystalline gypsum	M4	2.352	1.486	0.388	0.9177
	M5	2.380	1.729	0.274	0.8291
	Mean	2.366	1.607	0.331	
	St Dev	0.020	0.172	0.081	
General formula	Mean	2.320	1.440	0.545	
	St Dev	0.054	0.196	0.212	

Note: mean values and standard deviation for microcrystalline gypsum, macrocrystalline gypsum and for the entire dataset.

Please cite this article as: C. Caselle, S. Bonetto and C. Comina, Comparison of laboratory and field electrical resistivity measurements of a gypsum rock for mining prospection applications, International Journal of Mining Science and Technology, https://doi.org/10.1016/j.ijmst.2019.09.002

where a and m are material constants, related to the pore tortuosity and to the cementation respectively; and k the saturation exponent. Parameters a, m and k were estimated on the fitting of Archie's relationship on the experimental data for each sample (Fig. 5a); results are reported in Table 3.

Even if the Archie's parameters are similar for all the samples, a difference among microcrystalline and macrocrystalline samples is evident. Fig. 5b shows the measured resistivity values compared with the Archie's curves for microcrystalline and macrocrystalline gypsum and with a general curve, representative of the entire data set.

Using the mean values of a, m and k obtained for microcrystalline and macrocrystalline gypsum, porosity values were also estimated for each sample. Porosity estimations are referred to the mean values calculated with the resistivity data obtained in the different saturation conditions. Results are shown in Table 4. The comparison with the porosity values retrieved from dry/wet measurements shows the reliability of the proposed method and a good approximation of the chosen material constants. Overall porosity values of the sample remained quite stable independently from the textural composition of the sample (micro and macro).

Table 5 and Fig. 6 show the results of the mineralogical characterization of the gypsum samples. The range of gypsum content is high for all samples (above 85%) with a quite narrow variability range, suggesting a gypsum orebody potentially interesting from the economical point of view. The non-gypsum minerals have been recognized with XRPD analyses to be mainly calcite/Mg-calcite, quartz and minor clay minerals (Fig. 6).

Table 4
Comparison between porosity retrieved by resistivity measurements and by dry/wet measurements.

Porosity from dry/wet measurements	Porosity from archie formula
0.044	0.065 ± 0.020
0.074	0.077 ± 0.011
0.080	0.076 ± 0.013
0.051	0.061 ± 0.011
0.072	0.071 ± 0.014

Table 5
Gypsum content percentages for the 5 studied samples.

Sample	Gypsum content (%)
m1	91.83
m2	88.2
m3	86.6
M4	88.63
M5	95.25

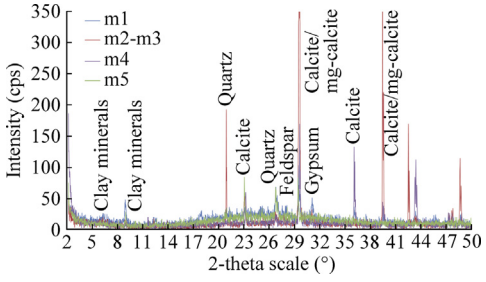

Fig. 6. XRPD analysis of the non-gypsum portions of the studied samples.

4.2. Field measurements

Fig. 7 shows two of the inverted ERT profiles acquired on field. Generally a good convergence of the inversion has been obtained for all the investigated profiles, with r.m.s. (root mean square) values always lower than 3.5%. Fig. 7 also shows three boreholes, drilled at short distance from the ERT lines (see also Fig. 2). The simplified stratigraphic columns were juxtaposed to the ERT profiles, to show the data correspondence.

The ERT profiles show a shallow layer with low resistivity values (10–15 Ω m) and thickness of approximately 20–25 m, interpreted as the marl and clay sediments at the top of the orebody. The lower limit of this layer is marked by a well-defined surface, almost sub-parallel to the ground surface, observable in the profiles. Below this surface, a new layer is present, with mean thickness of 40 m and higher resistivity, up to 100–150 Ω m. Given the corresponding stratigraphies obtained by the drillings, it is possible to consider this second layer as the gypsum orebody. These observations are common to all the investigated lines reported in Fig. 2. Moreover the longest lines (i.e. the lines shown in Fig. 7), with the greater investigation depths, locally allow to recognize also the lower limit of the gypsum orebody, highlighting the contact surface with the underlying clay and marl sediments. The depths of this limit obtained by ERT are acceptably coherent, considering the reduced resolution at depth, with drillings data.

5. Discussion

Laboratory results report measured resistivity values among 4000 and 400 Ω m, depending on the saturation condition, for the studied gypsum samples (Fig. 5b). Gypsum content for all the samples was observed to be always higher than 85% with very low percentage of clay minerals among the other constituents. In

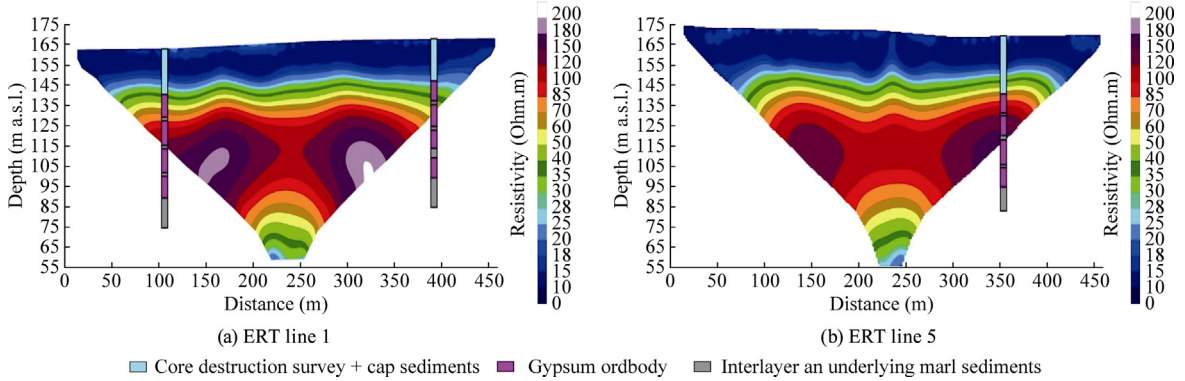

Fig. 7. Inversion results of the two principal ERT lines, with stratigraphic columns of nearby boreholes.

Please cite this article as: C. Caselle, S. Bonetto and C. Comina, Comparison of laboratory and field electrical resistivity measurements of a gypsum rock for mining prospection applications, International Journal of Mining Science and Technology, https://doi.org/10.1016/j.ijmst.2019.09.002

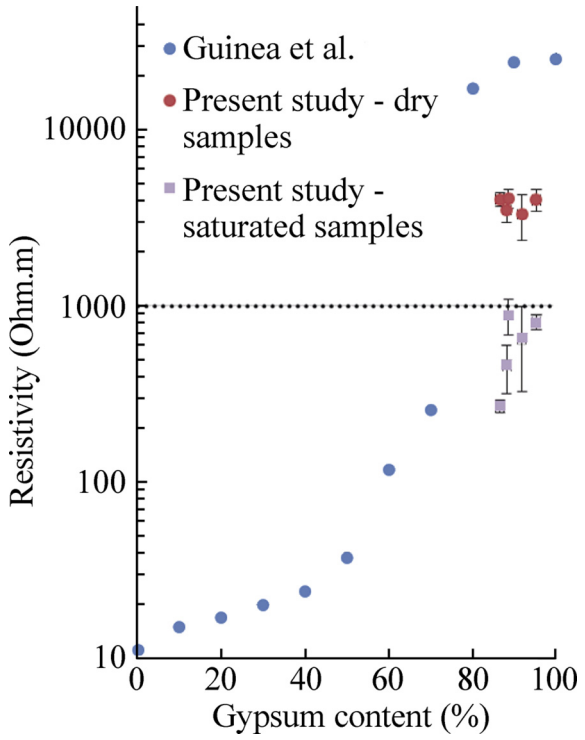

Fig. 8. Resistivity values obtained in this study compared with the resistivity vs gypsum content data from Guinea et al. [9].

dry conditions, the high measured resistivity values are therefore coherent with the high gypsum purity of the samples. Comparison with available literature data for dry gypsum samples are reported in Fig. 8 [9].

Our resistivity data on dry samples follow the trend suggested by the results reported in the study by Guinea et al. with a marked increase in resistivity above 80% gypsum content [9]. In the study by Guinea et al., even higher resistivity values are reported for samples with similar gypsum purity. Nevertheless, the authors considered these high resistivity values not reliable, neither representative, of the real field conditions, as it is evident from their geoelectrical classification (Table 1). The authors explained this incongruence with the field scale effect: the electrical current can find more conductive paths on field, due to the anisotropy of the field conditions, then in small scale samples. This will result in an increase in resistivity at the laboratory scale with the one at the field scale. In the same way, the difference in size and sample preparation between our work and the work in the study by Guinea et al. can explain the observed differences in the results. Natural samples, with their porosity, imperfections and heterogeneities, show obviously an higher propensity to create path for electrical current then sample-pills made with powdered gypsum and loaded under overpressure conditions (press machine at 200 kN) for 60 s, used in the study by Guinea et al. [9]. The lower resistivity measured in laboratory within this work in dry conditions can be also partially due to the measurement device adopted in this study (Fig. 4). Nevertheless, the adopted resistivity device offer the advantage of measuring directly on the gypsum sample and being very easy to use.

Even given these considerations, both dry datasets agrees in establishing a resistivity limit, around 1000 Ohm·m, separating gypsum contents lower and higher than 80%. Our data however also show that the resistivity of high purity gypsum samples is strongly dependent on the saturation conditions of the samples. Even for gypsum purity above 85% our measured resistivity values, in saturated conditions, are outside the ranges proposed in Table 1. This brings to the consideration that neglecting the saturation conditions in the measurements can bring to erroneous judgments on the features and quality of the investigated orebody. The proposed relationship (Fig. 5), calibrated to properly take into account this saturation effect, represent, to our knowledge, the first available correlation among electrical resistivity, saturation degree and porosity for gypsum rocks.

Despite the selected samples can be considered representative of the gypsum orebody in the test site, field and laboratory resistivity results does not completely agree. The gypsum resistivity value measured on field for the gypsum orebody (150 Ω m) is significantly lower than the one obtained in laboratory, even at full saturation condition. Again, following the geoelectrical classification proposed in Table 1, a quantitative evaluation of the gypsum purity based on the solely field ERT data would suggest a non-economic convenient exploitation. This conflicts with the observed gypsum content at the laboratory scale, always higher than 85%.

It has to be however considered that, with the interelectrode spacings adopted at the field scale (5–10 m), the resolution of the ERT method did not allowed the identification of each gypsum layer separately and of the interlayer marl layers among them (Fig. 7). Gypsum body is identified as a unique formation of about 40 m thickness which features are the result of the average of the four gypsum layers and of the three interlayer marl layers. The resulting average resistivity value reflects therefore the presence of the marls within the gypsum layers and leads to a reduced resistivity with respect to the one of the only gypsum, supposed in saturated condition.

With the aim to confirm these hypotheses and to verify the reliability of the results, a 2D electrical model was developed starting from the geological features at the site and from the stratigraphic information from the boreholes. This model is intended to replicate field measurements under known subsurface conditions. The ERT line in Fig. 7a was chosen as reference line, given the presence of 2 calibration boreholes to constrain depths and layering of the different geologic units.

The geoelectric model (Fig. 9a) was developed using the Res2dMod software, which incorporates the same forward algorithm used for inversion, and consists of:

(1) 0–15 m: fine sediments, clays and marls, with low resistivity (10 Ω m);
(2) 15–25 m: presence of thin layers and lenses of gypsum within the clay sediments that partially raise the resistivity (30 Ω m, following the electrical classification in the study by Guinea et al. [9]);
(3) 25–73 m: gypsum orebody, with 4 saturated gypsum layers (400 Ω m, following our laboratory data) and 3 interlayer marl levels (10 Ω m).
(4) from 73 m: bottom clay and marls with low resistivity (10 Ω m)

Gypsum layers reference resistivity was obtained considering the layers completely saturated, following the hydrogeological evidences in the area, with a constant water conductivity of 4.00 mS/cm [15]. The resulting resistivity value was obtained with the use of the equation proposed in Fig. 5b.

Over this model a forward simulation was performed reproducing the electrodes disposition and the array configuration used on field. The obtained data were then inverted with the same approach used for field data. The result of the inversion process of the modelled and measured data are shown in Fig. 9b and 9c respectively. The similarity between the two profiles confirms

Please cite this article as: C. Caselle, S. Bonetto and C. Comina, Comparison of laboratory and field electrical resistivity measurements of a gypsum rock for mining prospection applications, International Journal of Mining Science and Technology, https://doi.org/10.1016/j.ijmst.2019.09.002

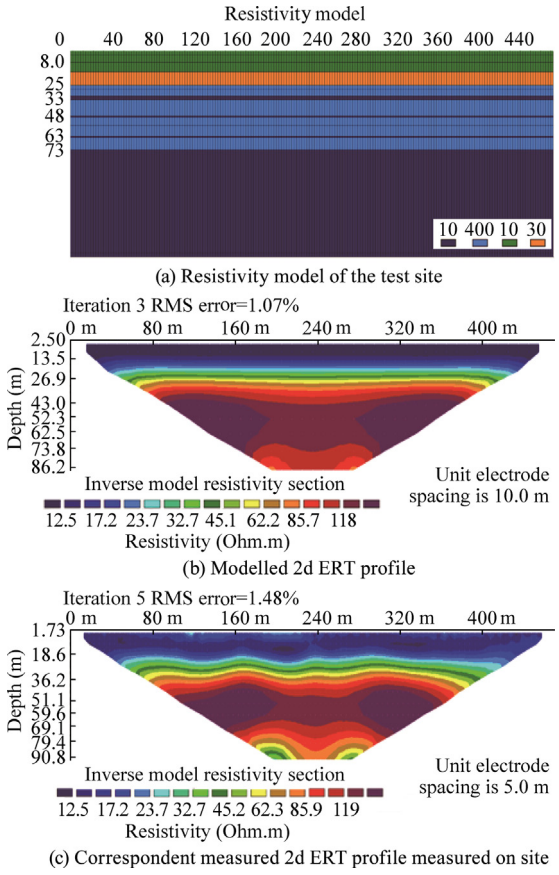

(a) Resistivity model of the test site

(b) Modelled 2d ERT profile

(c) Correspondent measured 2d ERT profile measured on site

Fig. 9. Comparison of modelled and measured inverted ERT profiles.

the geological and geoelectrical hypotheses considered to create the model.

The gypsum resistivity values along the ERT lines is therefore reduced with respect to the laboratory measurements because of:

(a) the saturation level and interstitial fluid properties, following the Archie's Formula;
(b) the presence of marl and clay interlayers whose low thickness inhibit the identification with the ERT but influence the global measured resistivity;
(c) the low resistivity of the cap materials, that influence the real resistivity of gypsum, reducing it. This effect is however partially compensated by the inversion process.

From the above reported analyses, a clear gypsum orebody with high purity saturated gypsum layers is therefore concluded to be present at the site. The application of the ERT surveys offers the additional advantage of a spatial reconstruction of its geometry. With this aim, ERT data along the survey lines have been interpolated with the Voxler software to obtain a 3d visualization of the upper surface of the orebody (Fig. 10) and a preliminary estimation of the exploitable volume. The resulting surface shows a good lateral continuity, with high correspondence among data from the different ERT profiles and from the drillings.

6. Conclusion

Considering the high variability of the electrical resistivity in gypsum ore bodies with similar geometrical and compositional features, this research aims at clarifying the significance of this variability with respect to specific features, such as composition and saturation, helping mining prospection and planning. In particular, a relationship between gypsum water saturation and electrical resistivity has been evaluated at the laboratory scale, considering typical values of water resistivity for the water-gypsum oversaturated solutions. Given the high dependence of the electrical measurements from the gypsum content, we selected gypsum rocks within a very tight gypsum percentage range. This relationship is, to our knowledge, the first available for this type of material. This relationship would be helpful in the preliminary hydrogeological reconstruction of the ore bodies, which is fundamental in mining activities to assure safety conditions and proper operational activities.

The possibility to retrieve the saturation of the material from the resistivity data opens the possibility to indirectly evaluate the porosity, another important parameter strongly influencing the mechanical behaviour of the rock and the mining design. With the use of the Archie's Formula, we estimated the material parameters and calculated the porosity for each sample. Obtained porosity values show a good correspondence with the ones retrieved from dry/wet measurements. Different material constants are proposed to describe gypsum samples with very different features, such as the microcrystalline branching selenite gypsum and the macrocrystalline massive selenite gypsum. Even if the differences in grain size, pore shape and size are significant, the parameters variability is not very significant: general parameters are also proposed that can be considered representative for all the considered data set and independent from the gypsum facies.

Field ERT data, with the help of a numerical simulation, were finally used to validate the relationship obtained in laboratory

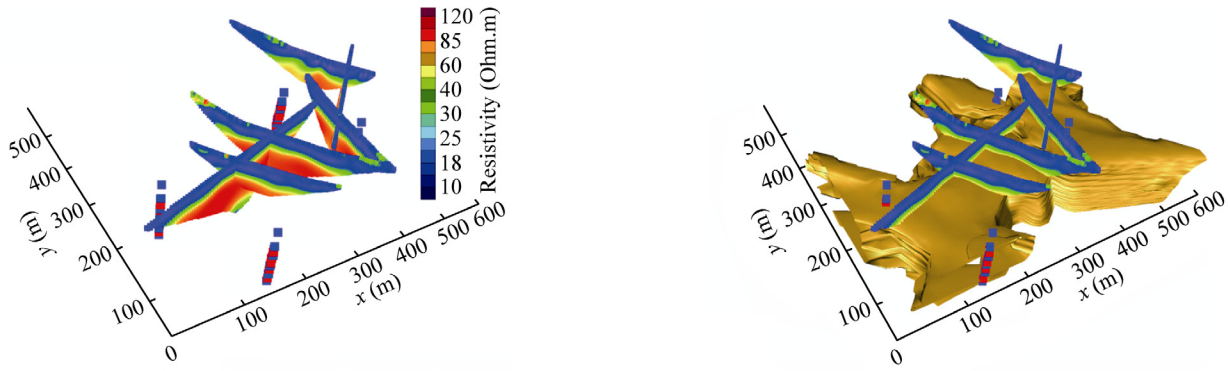

(a) 3d visualization of the ERT lines and of the boreholes performed in the test site

(b) Upper surface of the gypsum body, obtained by the interpolation of ERT profiles and boreholes information with Voxler software

Fig. 10. Three-dimensional visualization of all the ERT lines acquired in the test site.

Please cite this article as: C. Caselle, S. Bonetto and C. Comina, Comparison of laboratory and field electrical resistivity measurements of a gypsum rock for mining prospection applications, International Journal of Mining Science and Technology, https://doi.org/10.1016/j.ijmst.2019.09.002

and to attain a global representation of the orebody in the survey site.

The reliability of the proposed relationships open important scenarios in the interpretation of field data with geoelectrical prospection in evaporitic successions. The results of the research, combining easily executable resistivity laboratory measurements, with an on proper developed device, and field measurements, allowed a correct reconstruction of the orebody. The knowledge of the proposed relationships helps in the quantification of gypsum purity and the presence and the quantity of water within the rock orebody, that is often one of the most influencing parameters in the evaluation of the safety of the exploitation.

Acknowledgements

The Authors are indebted with the anonymous private company that kindly provided the drilling cores used in this study and financed the field surveys.

References

[1] Arai E. A resistivity tomography test survey in the Toyoha Mine, Hokkaido, Japan. Explor Geophys 1995;26(3):45–50.
[2] Maillol JM, Seguin MK, Gupta OP, Akhauri HM, Sen N. Electrical resistivity tomography survey for delineating uncharted mine galleries in West Bengal, India. Geophys Prospect 1999;47(2):103–16.
[3] Van Schoor. The application of in-mine Electrical Resistance Tomography (ERT) for mapping potholes and other disruptive features ahead of mining. J S Afr Inst Min Metall 2005;105(6):447–51.
[4] Saladich J, Rivero L, Queralt I, Lovera R, Font X, Himi M, et al. Geophysical evaluation of the volume of a mine tailing dump (Osor, Girona, NE Spain) using ERT. In: 22nd European meeting of environmental and engineering geophysics, near surface geoscience; 2016.
[5] Uhlemann SS, Chambers JE, Alonso AT, Gea D, Falck WE. Imaging of karst features to guide mining activities in a marble quarry by means of 3D ERT. In: Near surface geoscience 2015 - 21st European meeting of environmental and engineering geophysics; 2015. p. 711–5.
[6] Lugo E, Playà E, Rivero L. Aplicación de la tomografía eléctrica a la prospección de formaciones evaporíticas. Geogaceta 2008;44:223–6.
[7] Ball LB, Lucius JE, Land LA. Teeple AP. Geological Survey Scientific Investigations Report 2006. US Geological Survey; 2006.
[8] Guinea A, Playà E, Rivero L, Himi M. Electrical Resistivity Tomography and Induced Polarization techniques applied to the identification of gypsum rocks. Near Surf Geophys 2010;8(3):249–57.
[9] Guinea Ander, Elisabet P, Lluís R, Mahjoub H, Ricard B. Geoelectrical classification of gypsum rocks. Surv Geophys 2010;31(6):557–80.
[10] Guinea Ander, Elisabet P, Lluís R, Juan JL, Pilar Q. The electrical properties of calcium sulfate rocks from decametric to micrometric scale. J Appl Geophys 2012;85(10):80–91.
[11] Asfahani J, Mohamad R. Geo-electrical investigation for sulfur prospecting in Teshreen structure in Northeast Syria. Explor Min Geol 2002;11(1–4):49–59.
[12] Benson RC, Kaufmann RD. Characterization of a highway sinkhole within the gypsum karst of Michigan. In: Beck BF, Herring JG, editors. Geotechnical and environmental applications of karst geology and hydrology. Taylor & Francis; 2001. p. 103–12.
[13] Orellana E. Prospección geoeléctrica en corriente continua. Paraninfo; 1982.
[14] Martínez-Moreno FJ, Galindo-Zaldívar J, Pedrera AL, González-Castillo P, Ruano JM, Calaforra Guirado E. Detecting gypsum caves with microgravity and ERT under soil water content variations (Sorbas, SE Spain). Eng Geol 2015;193(7):38–48.
[15] Vigna Bartolomeo, Ilenia DA, Adriano F, Waele JD. Hydrogeological flow in gypsum Karst areas: some examples from Northern Italy and main circulation models. Int J Speleol 2017;46(2).
[16] Bonetto S, Fiorucci A, Fornaro M, Vigna B. Subsidence hazards connected to quarrying activities in a Karst Area: the case of the Moncalvo Sinkhole Event (Piedmont, NW Italy). Estonian J Earth Sci 2008;57(3):125.
[17] Giambastiani M. Soft rocks in Argentina. Int J Mining Sci Technol 2014;24 (6):883–92.
[18] Dela Pierre F, Natalicchio M, Lozar F, Bonetto S, Carnevale G, Cavagna S, et al. The Northermost record of the Messinian salinity crisis (Piedmont Basin, NW Italy). Geol Field Trips 2016;8:1–58.
[19] Pierre FD, Clari P, Natalicchio M, Ferrando S, Giustetto R, Lozar F, et al. Flocculent layers and bacterial mats in the mudstone interbeds of the primary lower gypsum unit (Tertiary Piedmont Basin, NW Italy): archives of palaeoenvironmental changes during the messinian salinity crisis. Mar Geol 2014;355(9):71–87.
[20] Marchianotti F. L'interazione dei grandi scavi in sotterraneo con gli acquiferi. PhD Thesis. Polytechnic of Turin; 2014.
[21] Lugli Stefano, Manzi V, Roveri M, Charlotte Schreiber B. The primary lower gypsum in the Mediterranean: a new facies interpretation for the first stage of the messinian salinity crisis. Palaeogeogr Palaeoclimatol Palaeoecol 2010;297 (1):83–99.
[22] Papadopoulos Z, Kolaiti E, Mourtzas N. The effect of crystal size on geotechnical properties of neogene gypsum in crete. Q J Eng Geol 1994;27 (3):267–73.
[23] Rupnow TD, Icenogle P. Evaluation of surface resistivity measurements as an alternative to the rapid chloride permeability test for quality assurance and acceptance. Baton Rouge (LA): Louisiana Department of Transportation; 2011. p. 68.
[24] Presuel-Moreno F, Liu Y, Paredes M. Concrete resistivity on the apparent surface resistivity measured via the four-point wenner method. In: Corrosion 2009, NACE International, Atlanta.
[25] Porta J. Methodologies for the analysis and characterization of gypsum in soils: a review. Geoderma 1998;87:31–46.
[26] Loke MH. Res2Dinv ver. 3.59 for Windows XP/Vista/7, 2010. Rapid 2-D Resistivity & IP Inversion Using the Least-Squares Method. Geoelectrical Imaging 2D & 3D Geotomo Software; 2010.
[27] Archie GE. The electrical resistivity log as an aid in determining some reservoir characteristics. Petrol Trans AIME 1942;146:54–62.
[28] Wang G, Qin Y, Shen J, Hu Y, Liu D, Zhao L. Resistivity response to the porosity and permeability of low rank coal. Int J Mining Sci Technol 2016;26 (2):339–44.
[29] Caselle C, Bonetto S, Vagnon F, Costanzo D. Dependence of Macro Mechanical Behaviour of Gypsum Rock on Micro-scale Grain-Size Distribution. Géotechnique Letters 2019. https://doi.org/10.1680/jgele.18.00206.
[30] Caselle C, Bonetto S, Colombero C, Comina C. Mechanical properties of microcrystalline branching selenite gypsum samples and influence of constituting factors. J Rock Mech Geotech Eng 2019;11(2):228–41. https://doi.org/10.1016/j.jrmge.2018.09.003.
[31] Caselle C, Umili G, Bonetto S, Ferrero AM. Application of DIC analysis method to the study of failure initiation in gypsum rocks. Géotechnique Letters 2019;9 (1):35–45. https://doi.org/10.1680/jgele.18.00156.
[32] Caselle C, Penone A, Bonetto S. Preliminary mechanical characterisation of gypsum rock using UCS and Point Load Test correlation. Geoingegneria Ambientale E Mineraria 2018;153:60–7.
[34] Caselle C, Bonetto S, Voagnon F, Costanzo D. Preliminary results of gypsum mechanical characterization. In: Litvinenko V, editor. Geomechanics and Geodynamics of Rock Masses. Presented at the EUROCK - ISRM Symposium 2018. Taylor & Francis Group; 2018. p. 1123–8.
[35] Caselle C, Umili G, Bonetto S, Constanzo D, Ferrero AM. Evolution of Local Strains Under Uniaxial Compression in an Anisotropic Gypsum Sample. In: Calvetti F, Cotecchia F, Galli A, Jommi C, editors. Geotechnical Research for Land Protection and Development. Springer; 2020. p. 454–61.
[36] Caselle C, Bonetto S, Comina C, Stocco S. Preliminary evaluation of In-mining GPR surveys for the identification of karst anomalies in a gypsum quarry. 1st Conference on Geophysics for Mineral Exploration and Mining, Near Surface Geoscience 2016. 2016.

Please cite this article as: C. Caselle, S. Bonetto and C. Comina, Comparison of laboratory and field electrical resistivity measurements of a gypsum rock for mining prospection applications, International Journal of Mining Science and Technology, https://doi.org/10.1016/j.ijmst.2019.09.002